European Journal of Nuclear Medicine and Molecular Imaging (2019) 46:1117–1131
https://doi.org/10.1007/s00259-018-4246-2

ORIGINAL ARTICLE

Testing the diagnostic accuracy of [18F]FDG-PET in discriminating spinal- and bulbar-onset amyotrophic lateral sclerosis

Arianna Sala[1,2] · Leonardo Iaccarino[1,2] · Piercarlo Fania[3] · Emilia G. Vanoli[4] · Federico Fallanca[4] · Caterina Pagnini[2] · Chiara Cerami[2,5] · Andrea Calvo[6] · Antonio Canosa[6] · Marco Pagani[7,8] · Adriano Chiò[6,7,9] · Angelina Cistaro[10] · Daniela Perani[1,2,4]

Received: 12 September 2018 / Accepted: 19 December 2018 / Published online: 7 January 2019

Abstract

Purpose The role for [18F]FDG-PET in supporting amyotrophic lateral sclerosis (ALS) diagnosis is not fully established. In this study, we aim at evaluating [18F]FDG-PET hypo- and hyper-metabolism patterns in spinal- and bulbar-onset ALS cases, at the single-subject level, testing the diagnostic value in discriminating the two conditions, and the correlations with core clinical symptoms severity.

Methods We included 95 probable-ALS patients with [18F]FDG-PET scan and clinical follow-up. [18F]FDG-PET images were analyzed with an optimized voxel-based-SPM method. The resulting single-subject SPM-t maps were used to: (a) assess brain regional hypo- and hyper-metabolism; (b) evaluate the accuracy of regional hypo- and hyper metabolism in discriminating spinal vs. bulbar-onset ALS; (c) perform correlation analysis with motor symptoms severity, as measured by ALS-FRS-R.

Results Primary motor cortex showed the most frequent hypo-metabolism in both spinal-onset (~57%) and bulbar-onset (~64%) ALS; hyper-metabolism was prevalent in the cerebellum in both spinal-onset (~56.5%) and bulbar-onset (~55.7%) ALS, and in the occipital cortex in bulbar-onset (~62.5%) ALS. Regional hypo- and hyper-metabolism yielded a very low accuracy (AUC $\leq$ 0.63) in discriminating spinal- vs. bulbar-onset ALS, as obtained from single-subject SPM-t-maps. Severity of motor symptoms correlated with hypo-metabolism in sensorimotor cortex in spinal-onset ALS, and with cerebellar hyper-metabolism in bulbar-onset ALS.

Conclusions The high variability in regional hypo- and hyper-metabolism patterns, likely reflecting the heterogeneous pathology and clinical phenotypes, limits the diagnostic potential of [18F]FDG-PET in discriminating spinal and bulbar onset patients.

Keywords Amyotrophic lateral sclerosis · Biomarkers · Diagnosis · [18F]FDG-PET · Brain metabolism

Introduction

Amyotrophic lateral sclerosis (ALS) is a fatal neurodegenerative disorder characterized by progressive degeneration of both upper and lower motor neurons (UMN, LMN) [1]. ALS diagnosis is currently based on the El Escorial revised criteria (EEC-R) [2]. According to the EEC-R criteria, diagnosis of ALS can be made when (i) evidence for progressive UMN and LMN degeneration is present, as shown by either clinical, neurophysiological or neuropathological examination

✉ Daniela Perani
perani.daniela@hsr.it

1 Vita-Salute San Raffaele University, Milan, Italy

2 In Vivo Human Molecular and Structural Neuroimaging Unit, Division of Neuroscience, IRCCS San Raffaele Scientific Institute, Milan, Italy

3 Positron Emission Tomography Centre IRMET, Affidea, Turin, Italy

4 Nuclear Medicine Unit, IRCCS San Raffaele Hospital, Via Olgettina, 60 Milan, Italy

5 Clinical Neuroscience Department, San Raffaele Turro Hospital, Milan, Italy

6 ALS Center, 'Rita Levi Montalcini' Department of Neuroscience, University of Turin, Turin, Italy

7 Institute of Cognitive Sciences and Technologies, C.N.R, Rome, Italy

8 Department of Nuclear Medicine, Karolinska Hospital, Stockholm, Sweden

9 Neuroscience Institute of Turin, Turin, Italy

10 Department of Neuroscience, Advisor Nuclear Medicine for Amiotrophic Lateral SclerosisRegional Expert Center, University of Turin, Turin, Italy

and (ii) lower motor neuron deficits are present, as defined by clinical examination or neurophysiological examination. Clinical diagnosis of ALS is usually delayed by one year after the patient's first referral [3, 4], a relatively long time considering that average survival of ALS patients is less than three years from symptom onset [5]. Notably, diagnosis of ALS is further complicated by the phenotypic heterogeneity of the disorder. Two-thirds of the patients present "patchy" LMN and UMN involvement with variable weakness of the limbs (spinal-onset ALS), whereas one-third of the patients present UMN and LMN involvement as expressed by bulbar muscles weakness, together with dysphagia and dysarthria (bulbar-onset ALS) [6]. Altogether, clinical heterogeneity and overlap between ALS and other motor neuron diseases contribute to a significant misdiagnosis rate in ALS, which is estimated to be around 45% [7–10].

Accuracy of clinical diagnosis might be improved by the use of neuroimaging biomarkers, which have been increasingly recognized of utmost importance in supporting clinical diagnosis in neurological degenerative conditions (e.g. [11–16]). Notwithstanding, the use of neuroimaging in ALS is currently limited to MRI of the brain and spinal cord [5], with its role however restricted only to the exclusion of other diseases that may mimic ALS [10]. Among molecular neuroimaging biomarkers, [18F]FDG-PET has been suggested as a supportive biomarker for ALS clinical diagnosis [1]. [18F]FDG-PET, a proxy for glucose metabolism in neurons, and specifically at synapses [17], is a well-established biomarker in neurodegenerative diseases [12–16, 18, 19], able to support early differential diagnosis [20–23], also in prodromal disease stages [22–27]. In ALS, previous [18F]FDG-PET studies reported some evidence for group-level hypometabolism in primary motor cortex, premotor cortex and dorsolateral frontal cortex, and hypermetabolism in the midbrain, pons and cerebellum [28–33]. Limited evidence, again only at group-level, suggests inconsistent patterns of hypo- and hypermetabolism characterizing spinal and bulbar clinical phenotypes in ALS [28, 29], with also one study reporting no significant differences between groups [30]. A recent single-subject analysis of the metabolic picture in ALS reports very heterogeneous profiles [31], prompting the need for further studies, particularly at the single-subject level. Crucially, the validation of [18F]FDG-PET as supportive biomarker for the diagnostic work-up in ALS depends on first establishing definite metabolic patterns for ALS sub-types [28].

This study aims at (i) characterizing, at the single-subject level, the [18F]FDG-PET patterns of hypo- and hypermetabolism in a large sample of patients with bulbar-onset and spinal-onset ALS, as assessed with an optimized SPM-based voxel-wise procedure [22]; (ii) testing the potential diagnostic value of [18F]FDG-PET biomarker metric, by evaluating its accuracy in discriminating spinal vs. bulbar-onset ALS; (iii) assessing the clinical significance of brain metabolism alterations in ALS, by testing the associations between clinical symptoms severity, as measured by an ad hoc functional scale, i.e. the ALS-Functional Rating Scale-Revised (ALS-FRS-R) scale, and [18F]FDG-PET metabolism.

Material and methods

Participants

Ninety-five patients with ALS were retrospectively collected from the clinical and neuroimaging databases of ALS Center, Turin (N = 86) and San Raffaele Hospital, Milan (N = 9). Patients had been referred to our research centers to perform the [18F]FDG-PET examination as part of research programs approved by the Ethical Committees.

The patients received a laboratory-supported, probable or definite ALS diagnosis according to the revised El Escorial ALS criteria [3]. The patients were classified according to their clinical presentation as either spinal ($n = 60$) or bulbar ($n = 35$)(see [28] for details). All patients underwent full neurological evaluation and an [18F]FDG-PET imaging session. Patients with primary lateral sclerosis (PLS), progressive muscular atrophy (PMA), spastic paresis, severe atrophy or vascular damage were excluded. Demographics, ALSFRS-R scores and neuropsychological classification for the whole ALS group and for spinal-onset and bulbar-onset subgroups are reported in Table 1.

[18F]FDG-PET acquisition and pre-processing

The [18F]FDG-PET scans were acquired at the Nuclear Medicine Department of Affidea Irmet Centre, Turin (N = 86) and at the Nuclear Medicine Unit of San Raffaele Hospital, Milan (N = 9), using a Discovery STE PET scanner (3.75 mm thickness; 5.2 mm in-plane FWHM; 3.27 mm thickness; 5.55 mm in-plane FWHM, respectively), manufactured by GE Healthcare. The [18F]FDG-PET acquisition procedures conformed to the European Association of Nuclear Medicine guidelines [34]. Notably, during the PET acquisition procedures subjects were with eyes closed.

All images were reconstructed using an ordered subset-expectation maximization algorithm. Attenuation correction was based on CT scans. Image pre-processing was performed using SPM software (http://www.fil.ion.ucl.ac.uk/spm/software/), running in Matlab (MathWorks Inc., Sherborn, MA, USA). Following validated procedures [22], each [18F]FDG-PET image was spatially normalized to a specific [18F]FDG-PET template in the MNI space [35]. Warped images were then spatially smoothed with an isotropic 3D Gaussian kernel (FWHM: 8–8-8 mm). Global mean scaling was applied to each image in order to account for between-subject uptake variability [36].

Table 1 Clinical and demographic characteristics of the ALS patients

Characteristic		ALS (N = 95)	Spinal-onset ALS (N = 60)	Bulbar-onset ALS (N = 35)	T score	*P* value
Males % (N)		57.9% (55)	68.3% (41)	40% (14)	–	–
Age at PET scan (years)		62.52 ± 12	60.63 ± 12	65.74 ± 14	1.88	0.06
Disease duration at PET scan (months)		14.65 ± 12	14.82 ± 13	14.37 ± 11	0.17	0.86
ALSFRS-R total score		39.74 ± 6.8	39.58 ± 6.3	40.03 ± 7.83	0.31	0.76
ALSFRS-R bulbar score		9.97 ± 2	11.02 ± 1.5	8.12 ± 2.1	7.82	<0.001
ALSFRS-R fine Motor score		9.47 ± 2.9	9.02 ± 3	10.26 ± 2.7	2.01	0.04
ALSFRS-R gross Motor score		8.95 ± 3	8.1 ± 3	10.44 ± 2.4	3.93	<0.001
ALSFRS-R respiratory score		11.37 ± 1.6	11.47 ± 1.5	11.21 ± 1.7	0.78	0.45
Cognitive classification[a]	*Normal*	43 (45.3%)	27 (45%)	16 (45.7%)	–	–
	Cognitive impairment	16 (16.8%)	13 (21.7%)	3 (8.6%)		
	Behavioural impairment	4 (4.3%)	3 (5%)	1 (2.9%)		
	Fronto-temporal dementia	2 (2.1%)	0 (0%)	2 (5.7%)		
	Non-classifiable impairment	6 (6.3%)	5 (8.3%)	1 (2.9%)		
	NA	24 (25.26%)	12 (20%)	12 (34.3%)		

[a] Extensive details on the cognitive classification of the subjects are provided in [32]

Optimized single-subject [18F]FDG-PET SPM analysis

[18F]FDG-PET processing was based on an optimized semi-quantitative procedure [22], validated in clinical research settings for differential diagnosis of various neurodegenerative conditions, including movement disorders [20, 26]. Following this validated procedure [22], the normalized and smoothed images were tested for relative whole-brain hypo-metabolism and hyper-metabolism by means of a two-sample t-test implemented in SPM, in which the single image was compared with a large ($N = 112$) normal control [18F]FDG-PET dataset, extensively described elsewhere [22]. Age was entered as a nuisance covariate. Taking into account the lack of reported differences in metabolic activity of male and female ALS patients, gender was not controlled for in the analysis. Of note, gender distribution did not differ between normal control and ALS groups ($\chi^2 = 2.303$, $p = .121$). For the assessment of hyper-metabolism, we set the grey matter threshold at 1.0, thus minimizing the risk of artefactual hyper-metabolism and improving the reliability of findings [29]. The resulting SPM-t-maps, thresholded at $P < 0.05$ family-wise error (FWE)-corrected for multiple comparisons (Ke: 250 voxels), represented the basis for (i) the assessment of the profiles of regional hypo- and hyper-metabolism in spinal- and bulbar-onset ALS and (ii) the evaluation of the diagnostic discriminative ability of regional hypo- and hyper-metabolism, as based on the SPM-t-maps.

ROIs for hypo- and hyper-metabolism

In order to characterize the hypo- and hyper-metabolism profiles of spinal- and bulbar-onset ALS, we further selected a series of regions of interest (ROIs) based on previous literature, including regions involved in ALS pathophysiology and/or reported as hypo- or hyper-metabolic in ALS [28–32](see Tables 2 and 3). ROIs were mainly derived from the Automated Anatomical Labelling Atlas (AAL) [37]. Due to the relative coarseness in the AAL ROIs, especially pertaining to the sensori-motor system of crucial relevance for ALS, we complemented the selected AAL ROIs with a set of more refined ROIs, derived from dedicated atlases or, if unavailable, manually drawn following specific guidelines, as follows: the dorsolateral prefrontal cortex, obtained from the Sallet's Dorsal Frontal Parcellation Atlas [38]; the pre-motor, primary motor and somatosensory cortices, derived from the Juelich Histological Atlas, as available in FMRIB Software Library (FSL), the supplementary pre-motor and motor area, which were manually drawn on a T1 high-resolution template following guidelines by Mayka et al. (2006) [39]; dorsal caudate, dorsal putamen and ventral striatum, delineated following guidelines by Tziortzi and colleagues (2011) [40]; the mesencephalon and pons, which were derived from the WFUPickAtlas Tailarach Daemon Lobar Atlas [41–43]; and the cerebellar nuclei, manually drawn following guidelines by Diedrichsen et al. (2011) [44]. The resulting ROIs were then projected on a T1 high-resolution MNI space template to check for any mismatch with known anatomical boundaries or presence of any overlap across different ROIs. For each patient, ROIs were deemed hypo- or hyper-metabolic when at least 50 significantly hypo- or hyper-metabolic voxels (as defined from the single-subject hypo−/hyper-metabolism SPM-t-maps) fell within the ROIs' boundaries. Percentage prevalence of each regional hypo- and hyper-metabolism was computed for each ALS sub-group. Percentage prevalence values in the two sub-groups were contrasted directly by means of a chi-squared test.

Table 2 Prevalence of regional hypo-metabolism in spinal-onset and bulbar-onset ALS

Macroarea	Selected ROIs	Prevalence of hypo-metabolism (%)		*p*-values[a]
		Spinal-onset ALS	Bulbar-onset ALS	
Frontal lobe	L DLPFC	31.67	45.71	n.s.
	R DLPFC	23.33	45.71	0.024[b]
	L Medial Superior Frontal Gyrus	21.67	40	n.s.
	R Medial Superior Frontal Gyrus	23.33	28.57	n.s.
	L Anterior Cingulate Cortex	20	45.71	<0.001
	R Anterior Cingulate Cortex	18.33	22.86	n.s.
	L Orbitofrontal Cortex	28.33	37.14	n.s.
	R Orbitofrontal Cortex	26.67	28.57	n.s.
	L Frontal Operculum	26.67	42.86	n.s.
	R Frontal Operculum	21.67	37.14	n.s.
Sensorimotor cortices	L Pre-motor Cortex	41.67	**51.43**	n.s.
	R Pre-motor Cortex	35	45.71	n.s.
	L Supplementary Pre-motor Area	33.33	45.71	n.s.
	R Supplementary Pre-motor Area	38.33	**57.14**	n.s.
	L Supplementary Motor Area	31.67	40	n.s.
	R Supplementary Motor Area	38.33	40	n.s.
	L Primary Motor Cortex	**56.67**	**71.43**	n.s.
	R Primary Motor Cortex	**58.33**	**57.14**	n.s.
	L Somatosensory Cortex	41.67	**54.29**	n.s.
	R Somatosensory Cortex	36.67	37.14	n.s.
Parietal lobe	L Inferior Parietal Lobule	35	31.43	n.s.
	R Inferior Parietal Lobule	11.67	22.86	n.s.
	L Superior Parietal Lobule	20	22.86	n.s.
	R Superior Parietal Lobule	21.67	28.57	n.s.
	L Posterior Cingulate Cortex	5	2.86	n.s.
	R Posterior Cingulate Cortex	1.67	5.71	n.s.
Occipital lobe	L Lateral Occipital Cortex	26.67	28.57	n.s.
	R Lateral Occipital Cortex	33.33	34.29	n.s.
	L Medial Occipital Cortex	28.33	25.71	n.s.
	R Medial Occipital Cortex	25	5.71	0.018[b]
Temporal lobe	L Fusiform Gyrus	26.67	40	n.s.
	R Fusiform Gyrus	23.33	20	n.s.
	L Inferior Temporal Gyrus	31.67	34.29	n.s.
	R Inferior Temporal Gyrus	25	37.14	n.s.
	L Middle Temporal Gyrus	13.33	20	n.s.
	R Middle Temporal Gyrus	36.67	48.57	n.s.
	L Superior Temporal Gyrus	21.67	17.14	n.s.
	R Superior Temporal Gyrus	31.67	48.57	n.s.
	L Temporal Pole	23.33	37.14	n.s.
	R Temporal Pole	31.67	**51.43**	n.s.
	L Parahippocampal Gyrus	20	22.86	n.s.
	R Parahippocampal Gyrus	16.67	20	n.s.
	L Hippocampus	11.67	14.29	n.s.
	R Hippocampus	15	14.29	n.s.
Insular cortex	L Insular Cortex	35	54.29	n.s.
	R Insular Cortex	28.33	37.14	n.s.
Subcortical structures	L Dorsal Caudate Nucleus	10	5.71	n.s.

Table 2 (continued)

Macroarea	Selected ROIs	Prevalence of hypo-metabolism (%)		*p*-values[a]
		Spinal-onset ALS	Bulbar-onset ALS	
	R Dorsal Caudate Nucleus	6.67	0	n.s.
	L Dorsal Putamen	13.33	5.71	n.s.
	R Dorsal Putamen	13.33	5.71	n.s.
	L Globus Pallidus	11.67	5.71	n.s.
	R Globus Pallidus	13.33	2.86	n.s.
	L Ventral Striatum	11.67	8.57	n.s.
	R Ventral Striatum	16.67	5.71	n.s.
	L Thalamus	18.33	11.43	n.s.
	R Thalamus	11.67	8.57	n.s.
Cerebellum	L Cerebellar Cortex	25	34.29	n.s.
	R Cerebellar Cortex	31.67	40	n.s.
	L Cerebellar Nuclei	16.67	20	n.s.
	R Cerebellar Nuclei	5	14.29	n.s.
	Vermis	21.67	31.43	n.s.

Prevalences of hypo-metabolism exceeding 50% are denoted in bold

[a] *p*-values refer to the significant differences in hypometabolism prevalence in the selected ROIs

[b] Not surviving Bonferroni correction for multiple comparisons

Discriminative analysis of regional hypo- and hyper-metabolism

First, we tested whether hypo- and hyper-metabolism alterations in each *single* brain region would allow to satisfactorily classify spinal- vs. bulbar-onset ALS.

Second, we tested whether *combining* regional hypo- and hyper-metabolism alterations in 67 brain regions (the same included in the former analyses) would improve discrimination between sub-groups. Following the most common approaches adopted in previous ALS studies (e.g. [28, 30, 45]), we performed a discriminant analysis and a support vector machine analysis (SVM) using a non-linear classifier with radial basis function kernel. A leave-one-out cross-validation, in which each case was classified by the function derived from all cases apart from the case itself, was performed in both analysis.

For all the above, discriminative performance was evaluated by means of an ROC curve analysis, considering the diagnosis at follow-up as the reference standard.

ROI metabolic distribution in the primary motor cortex

Considering that the difference between spinal- and bulbar- onset ALS is essentially related to the body part initially involved, we performed a precise study of the metabolism distribution in the primary motor cortex. ROIs corresponding to sub-regions of the primary motor cortex were drawn in accordance with [46]. In particular, we drew nine 5x5x5 mm^3 bilateral cubic seed ROIs, starting from the dorsomedial region of the primary motor cortex (foot/leg area), passing through the dorsolateral region (the hand/arm area) and ending in the ventrolateral region (face/head area and tongue area) (see [46]). ROIs pertaining to the same area were merged together, obtaining a total of four ROIs. For each patient, ROIs were deemed hypo- or hyper-metabolic when at least 50 significantly hypo- or hyper-metabolic voxels (as defined from the single-subject hypo−/hyper-metabolism SPM-t-maps) fell within the ROIs' boundaries. Percentage prevalence of each regional hypo- and hyper-metabolism was computed for each ALS sub-group and association between presence of metabolic alterations and type of onset was computed by means of a chi-squared test.

Clinico-metabolic correlations

A multiple regression approach was adopted to test the correlation, at group level, between brain glucose metabolism and clinical symptoms severity in the motor, bulbar and respiratory domain, as assessed by ALSFRS-R sub-scales scores. Multiple regression models were run separately for spinal- and bulbar-onset ALS sub-groups, entering age-adjusted individual SPM hypo- and hypermetabolism contrast images

Table 3 Prevalence of regional hyper-metabolism in spinal-onset and bulbar-onset ALS

Macroarea	Selected ROIs	Prevalence of hyper-metabolism		*p*-values[a]
		Spinal-onset ALS	Bulbar-onset ALS	
Sensorimotor cortices	L Pre-motor Cortex	26.67	20	n.s.
	R Pre-motor Cortex	41.67	37.14	n.s.
	L Supplementary Pre-motor Area	23.33	11.43	n.s.
	R Supplementary Pre-motor Area	41.67	37.14	n.s.
	L Supplementary Motor Area	15	22.86	n.s.
	R Supplementary Motor Area	21.67	25.71	n.s.
	L Primary Motor Cortex	43.33	40	n.s.
	R Primary Motor Cortex	45	**51.43**	n.s.
	L Somatosensory Cortex	30	40	n.s.
	R Somatosensory Cortex	48.33	**57.14**	n.s.
Occipital lobe	L Lateral Occipital Cortex	48.33	**71.43**	0.028[b]
	R Lateral Occipital Cortex	43.33	**54.29**	n.s.
	L Medial Occipital Cortex	41.67	**71.43**	0.005[b]
	R Medial Occipital Cortex	31.67	**54.29**	0.030[b]
Subcortical structures	L Dorsal Caudate Nucleus	6.67	5.71	n.s.
	R Dorsal Caudate Nucleus	0	2.86	n.s.
	L Dorsal Putamen	20	25.71	n.s.
	R Dorsal Putamen	23.33	25.71	n.s.
	L Globus Pallidus	13.33	14.29	n.s.
	R Globus Pallidus	11.67	20	n.s.
	L Ventral Striatum	30	34.29	n.s.
	R Ventral Striatum	1.67	31.43	n.s.
	L Thalamus	11.67	17.14	n.s.
	R Thalamus	15	37.14	0.014[b]
	Mesencephalon	18.33	34.29	n.s.
	Pons	11.67	11.43	n.s.
Cerebellum	L Cerebellar Cortex	**53.33**	**57.14**	n.s.
	R Cerebellar Cortex	**60**	**54.29**	n.s.
	L Cerebellar Nuclei	40	40	n.s.
	R Cerebellar Nuclei	41.67	42.86	n.s.
	Vermis	0	37.14	n.s.

[a] *p*-values refer to the significant differences in hyper-metabolism prevalence in the selected ROIs

[b] Not surviving Bonferroni correction for multiple comparisons

Prevalences of hyper-metabolism exceeding 50% are denoted in bold

(as derived by the single-subject [18F]FDG-PET SPM pipeline) and ALSFRS-R scores at gross- and fine-motor, bulbar and respiratory sub-scales as variables of interest; disease duration, defined as the time-course between the appearance of the earliest clinical symptom as reported by the patient and the [18F]FDG-PET scan, was entered as nuisance covariate. For this correlative analysis, we set a more liberal statistical threshold of $p < 0.001$, minimum cluster extent k:100 voxels ($p < 0.05$ FWE-corrected at cluster level), as a reasonable trade-off between statistical robustness and sensitivity [47].

Results

Regional hypo- and hyper-metabolism profiles

Illustrative examples of hypo- and hyper-metabolism patterns in ALS patients are presented in Figs. 1 and 2. Prevalence of regional hypo- and hyper-metabolism in spinal- and bulbar-onset ALS are reported in Tables 2 and 3. As clearly shown, hypo- and hyper-metabolism profiles partially overlapped across the two sub-groups. Primary motor cortex hypometabolism was maximally prevalent in both spinal-onset (L: 56.67%; R: 58.33%; L-R Average: 57.5%) and

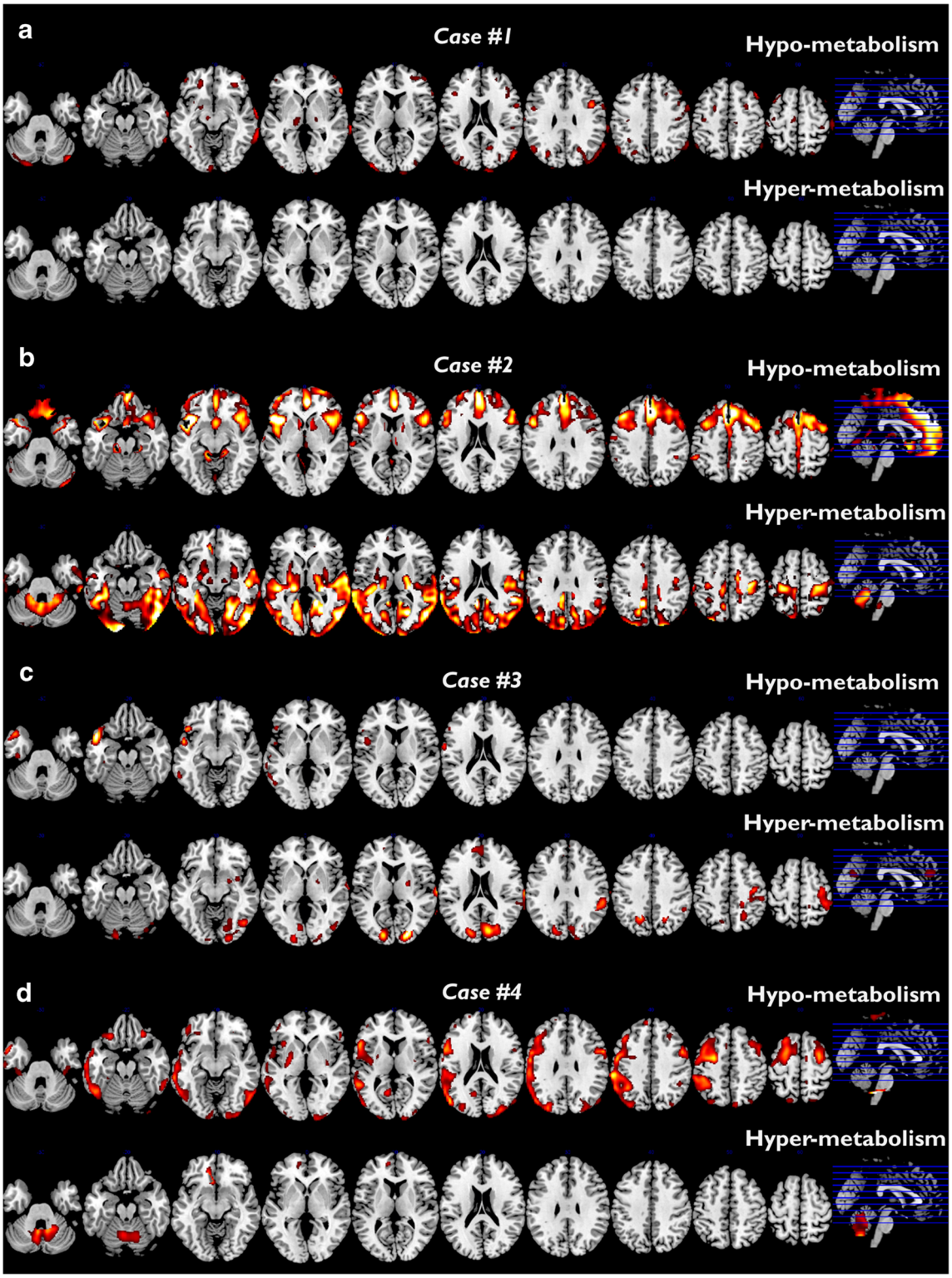

Fig. 1 Illustrative examples of brain hypo- and hyper-metabolism SPM-t-maps at the single-subject level in spinal-onset ALS cases showing the variability of hypo- and hyper-metabolism at [18F]FDG-PET SPM-t-maps in single subjects with spinal-onset ALS. (**a**) Normal brain metabolism in a male patient (age 58 years) with ALSFRS-R total score: 42. (**b**) Extensive frontal hypo-metabolism and occipito-cerebellar hyper-metabolism in a male patient (age 61 years) with executive deficits and ALSFRS-R total score: 42. (**c**) No hypometabolism, but occipital hyper-metabolism in a female patient (age 77 years) with ALSFRS-R total score: 40. (**d**) Extensive cortical and subcortical (pallidal) hypo-metabolism, with marked leftward asymmetry, and cerebellar hyper-metabolism in a female patient (age 67 years), with ALSFRS-R total score: 23. [18F]FDG-PET SPM-t-maps were estimated from comparison with a large dataset of 112 healthy controls, following validated procedures (see text for details). Statistical threshold was set at $p < 0.05$ FWE-corrected for multiple comparison at the voxel level; minimum cluster extent Ke: 250 voxels

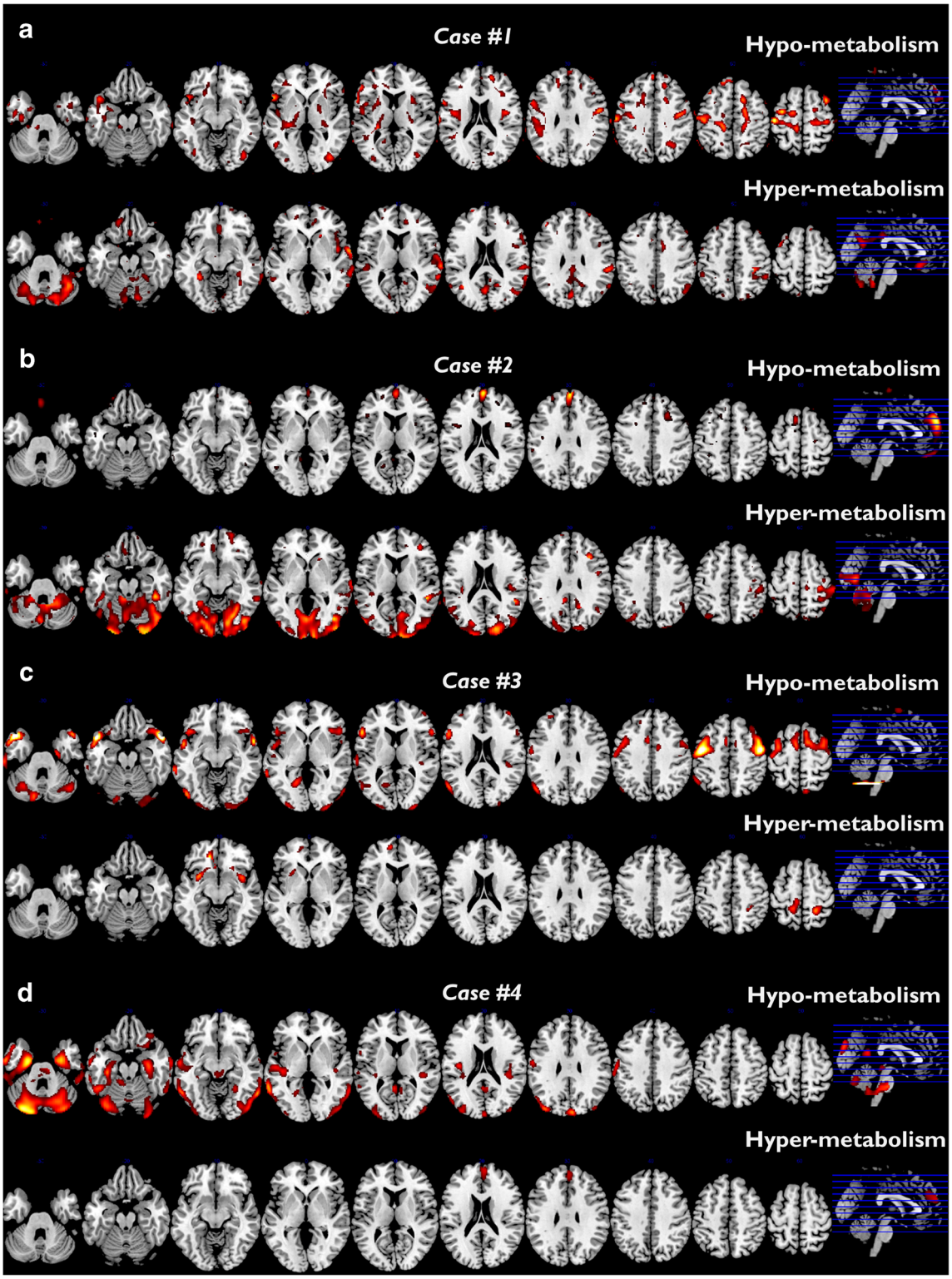

Fig. 2 Illustrative examples of brain hypo- and hyper-metabolism SPM-t-maps at the single-subject level in bulbar-onset ALS cases showing the variability of hypo- and hyper-metabolism at [18F]FDG-PET SPM-t-maps in single subjects with bulbar-onset ALS. (**a**) Circumscribed motor cortex hypo-metabolism and cerebellar hyper-metabolism in a female patient (age 78 years), with ALSFRS-R total score: 45. (**b**) No hypo-metabolism and occipito-cerebellar hyper-metabolism in a female patient (age 43 years), with ALSFRS-R total score: 43. (**c**) Fronto-temporal hypo-metabolism and no hyper-metabolism in a male patient (age 74 years), with fronto-temporal dementia and ALSFRS-R total score: 44. (**d**) Cerebellar, brainstem and temporal hypo-metabolism and no hyper-metabolism in a female patient (age 68 years), with ALSFRS-R total score: 47. [18F]FDG-PET SPM-t-maps were estimated from comparison with a large dataset of 112 healthy controls, following validated procedures (see text for details). Statistical threshold was set at $p < 0.05$ FWE-corrected for multiple comparison at the voxel level; minimum cluster extent Ke: 250 voxels

bulbar-onset (L: 71.43%; R: 57.14%; L-R Average: 64.29%) ALS. Cerebellar hyper-metabolism was maximally prevalent in spinal-onset ALS (L: 53.33%; R: 60%; L-R Average: 56.66%) but also reported in bulbar-onset ALS (L: 57.14%; R: 54.29%; L-R average: 55.72%), where the maximal prevalence was reached by hyper-metabolism in the lateral and medial occipital cortex (L: 71.43%; R: 54.29%; L-R average: 62.86%).

Performance of discriminative analysis of regional hypo- and hyper-metabolism

No specific metabolic hallmark emerged to discriminate spinal-onset vs. bulbar-onset ALS. Of note, a predominant hypo-metabolism in the left anterior cingulum was observed in bulbar-onset, as compared to spinal-onset ALS ($\chi^2 = 7.032$, $p < 0.001$), surviving Bonferroni-correction for multiple comparison (Table 2). This difference was however too weak to allow satisfactory discrimination across sub-groups, yielding low AUC levels (AUC = 0.63). No significant association was found between hypo-metabolism in the anterior cingulum and cognitive or behavioral deficits, although results of these statistical analyses might have been hampered by the limited availability of neuropsychological data in our sample (Table 1). Remaining significant differences in regional hypo- and hyper-metabolism (Tables 2 and 3) did not survive correction for multiple comparisons.

Discrimination between sub-groups when using multivariate methods remained unsatisfactory. Following cross-validation, the discriminant analysis was able to correctly classify 18/35 (51.43%) of bulbar-onset and 39/60 (65%) of spinal-onset cases, thus reaching an AUC of 0.59. The SVM, applied by radial basis function kernel, failed to discriminate bulbar-onset vs. spinal-onset ALS (sensitivity = 0%). When testing other linear and non-linear classifiers with SVM, again followed by leave-one-out cross-validation, the best performance was achieved when using a polynomial kernel, correctly classifying 12/35 (34.28%) of bulbar-onset and 51/60 (85%) of spinal-onset cases, thus reaching an AUC of 0.60.

ROI metabolic distribution in the primary motor cortex

Prevalence of hypo- and hyper-metabolism alterations in sub-regions of the primary motor cortex is reported in Table 4. Highest prevalence of metabolic alterations was found in the foot/leg and hand/arm areas in spinal-onset ALS (hypometabolism prevalence: L: 25%; R: 26.67%; L-R Average: 25.84%, L: 25%; R: 23.33%; L-R Average: 24.16%, respectively) and in the face/head and hand/arm areas in bulbar-onset ALS (hypometabolism prevalence: L: 25.71%; R: 31.43%; L-R Average: 28.57%, L: 34.29%; R: 28.57%; L-R Average: 31.43%, respectively).

We found a significant association between hypo-metabolism in the right dorsomedial region (foot/leg area) and spinal-onset ALS ($\chi^2 = 4.52$, $p < 0.05$), and hypo-metabolism in the right ventrolateral region (face/head area) and bulbar-onset ALS ($\chi^2 = 4.52$, $p < 0.05$). These significant differences, however, did not survive correction for multiple comparisons.

Table 4 Prevalence of regional hypo- and hyper-metabolism in primary motor cortex areas in spinal-onset and bulbar-onset ALS

Prevalence type	Primary Motor Cortex Area	Spinal-onset ALS	Bulbar-onset ALS	*p*-values[a]
Prevalence of hypo-metabolism (%)	L foot/leg area	25	25.71	n.s.
	R foot/leg area	26.67	8.57	0.034[b]
	L hand/arm area	25	34.29	n.s.
	R hand/arm area	23.33	28.57	n.s.
	L face/head area	15	25.71	n.s.
	R face/head area	13.33	31.43	0.034[b]
	L tongue area	3.33	0	n.s.
	R tongue area	0	5.71	n.s.
Prevalence of hyper-metabolism (%)	L foot/leg area	11.67	14.29	n.s.
	R foot/leg area	6.67	14.29	n.s.
	L hand/arm area	20	11.43	n.s.
	R hand/arm area	11.67	8.57	n.s.
	L face/head area	20	17.14	n.s.
	R face/head area	16.67	11.43	n.s.
	L tongue area	15	22.86	n.s.
	R tongue area	6.67	5.71	n.s.

[a] *p*-values refer to the significant differences in hypo- and hyper-metabolism prevalence in the selected ROIs

[b] Not surviving Bonferroni correction for multiple comparisons

Clinico-metabolic correlations

Results of the clinico-metabolic correlation analyses are reported in Fig. 3. Different patterns of clinico-metabolic correlations emerged across the two sub-groups ($p < 0.001$ at voxel-level, $P < 0.05$ FWE-correct at cluster-level). In the spinal-onset ALS sub-group, we found a significant negative correlation ($R = -0.54$, $p < 0.001$) between brain hypo-metabolism contrast values in sensorimotor cortices, i.e. precentral and postcentral gyrus, and paracentral lobule, bilaterally, and ALSFRS-R Gross Motor Score (i.e. the more severe the *hypo*-metabolism, the more severe the motor symptoms). In bulbar-onset ALS, ALSFRS-R Gross Motor Score was again negatively correlated ($R = -0.60$, $p < 0.001$) with hyper-metabolism contrast values in cerebellar vermis and in the posterior portions of the right cerebellar cortex (lobule VIII/IX), i.e. the more severe the *hyper*-metabolism, the more severe the motor symptoms.

No significant correlations were reported for the remaining ALSFRS-R sub-scales, possibly due to ceiling effects (e.g. ALSFRS-R Respiratory sub-scale). After removing disease duration—as nuisance covariate—from the model, results remained substantially unchanged, with slightly more extended significant clusters, but still topographically identical to those shown in Fig. 3.

Discussion

A large body of studies has provided consistent evidence for the existence of highly specific patterns of brain hypo-metabolism in neurodegenerative diseases, as measured by [18F]FDG-PET [20–26]. Recently, a diagnostic role for [18F]FDG-PET in the diagnosis of ALS has been suggested [1], based on data from investigations reporting a fairly high accuracy in discriminating patients with ALS from healthy controls [28, 30]. Considering the challenges posed by ALS diagnosis, there is an urgent need to provide evidence for a possible role of [18F]FDG-PET as a biomarker for the differential diagnosis.

Regional hypo- and hyper-metabolism profiles in ALS sub-types

In this study we characterized, for the first time at the single-subject level, the patterns of regional hypo- and hyper-metabolism in spinal- and bulbar-onset ALS.

Hypometabolism in the primary motor cortex was the most consistent finding across single individuals in both sub-groups (Table 2), supporting previous [18F]FDG-PET evidence at the group level [28, 30, 31, 48]. This finding is also consistent with in vivo MRI data indicating a relative cortical thinning in the primary motor cortex in ALS [49], as well as with results of *postmortem* examinations in case series with familial and sporadic ALS that revealed a profound degeneration of apical dendrites in the pyramidal neurons of the primary motor cortex [50]. Notably, we found a significant association (although not surviving correction for multiple comparisons) between the topography of hypometabolism in the primary motor cortex and the type of disease onset, namely, hypo-metabolism in the right dorsomedial region (foot/leg area) for spinal-onset, and in right ventrolateral region (face/head area) for bulbar-onset ALS subtype. Altogether, these findings are compatible with the "dying forward" hypothesis of ALS [51, 52] according to which neurodegeneration and synaptic loss in cortical motor neurons could actively contribute to vulnerability of upper motor neurons in ALS, and not simply be the endpoint of a "dying back" phenomena directed from the neuromuscular junction towards the cerebral cortex [51, 53].

As for hyper-metabolism, the cerebellar cortex was predominantly involved in both sub-groups, with a high prevalence of occipital hyper-metabolism as well, consistent with previous group-level findings [28–31] (Table 3). Different mechanisms have been suggested as the basis of [18F]FDG-PET hyper-metabolism in ALS. For example, hyper-metabolism might be related to neuroinflammatory processes [28, 29]. Both reactive astrocytosis [54, 55] and microglial activation [55, 56] have been reported in ALS. Considering that, in areas of activated microglia, glucose metabolism increases of about 60%, as shown in vivo following induced ischemia in rat models [57], it stands to reason that microglia activation might result in enhanced glucose metabolism. As an alternative hypothesis, hyper-metabolism might stem from the loss of inhibitory inter-neuronal input, leading to neuronal overstimulation and excitotoxicity via calcium-mediated abnormal glutamatergic activity [58]. Since glutamatergic neurotransmission is the main determinant of cortical glucose consumption [59], increased glutamatergic activity might cause regional glucose hyper-metabolism, at least in the early diseases phases, when neurodegeneration has not yet fully occurred.

When testing for differences in spinal- and bulbar-onset sub-types, we found a higher prevalence of metabolic alterations in extra-motor regions associated with the bulbar-onset sub-type, consistent with some previous [18F]FDG-PET findings [29] and in support of the reported association between bulbar-onset and executive cognitive deficits [60] (Tables 2, 3).

Evaluation of [18F]FDG-PET as supportive biomarker in the diagnostic work-up of ALS

Of note, no specific spinal- or bulbar-onset signature was observed with the [18]FDG-PET SPM analysis. Crucially, metabolic alterations were assessed here with an optimized semi-quantitative univariate procedure [22] that allows

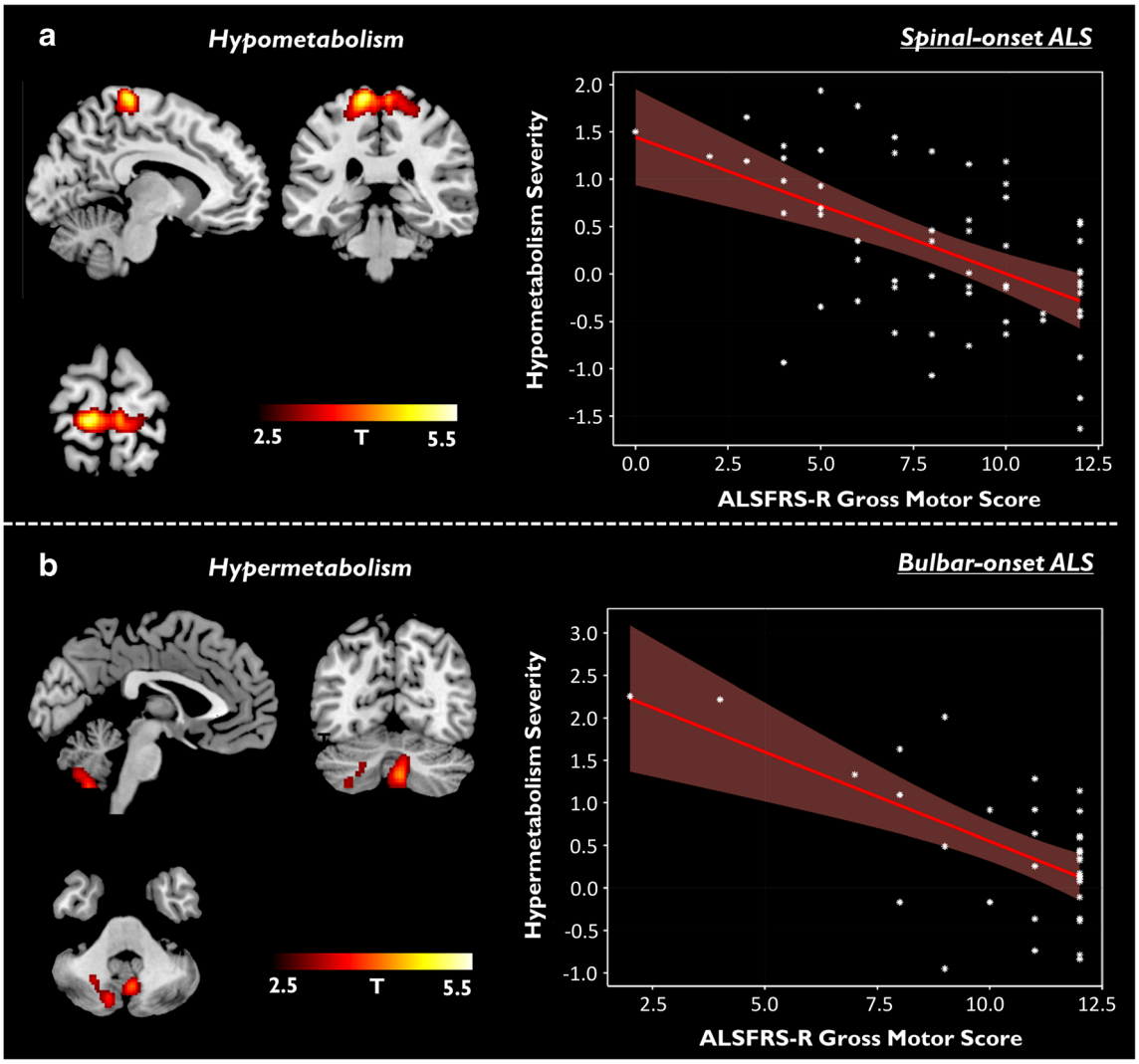

Fig. 3 Voxel-wise correlation between ALSFRS-R Gross Motor score and metabolic alterations in spinal- and bulbar-onset ALS. (**a**) Results of the voxel-based correlation analysis between ALSFRS-R Gross Motor score and [18F]FDG-PET brain glucose hypo-metabolism contrast values in ALS patients with spinal-onset, covarying for age, sex and disease duration. A significant negative correlation ($R = -0.54$, $p < 0.001$) was found between ALSFRS-R Gross Motor score and hypo-metabolism in sensorimotor cortices (left panel), i.e. the more severe the motor symptoms, the more severe the hypo-metabolism. The graph shows the correlation between ALSFRS-R Gross Motor score (x axis) and the average SPM hypo-metabolism contrast values in the sensorimotor cluster (y axis) (*right panel*). Positive SPM contrast values (y axis) indicate lower-than-HC brain glucose metabolism, and vice-versa. *Red shaded areas* represent confidence intervals for the regression line slope. (**b**) Results of the voxel-based correlation analysis between ALSFRS-R Gross Motor score and [18F]FDG-PET brain glucose hyper-metabolism contrast values in ALS patients with bulbar-onset, covarying for age, sex and disease duration. A significant negative correlation ($R = -0.60$, $p < 0.001$) was found between ALSFRS-R Gross Motor score and hyper-metabolism in cerebellar vermis and cortex (*left panel*), i.e. the more severe the motor symptoms, the more severe the hyper-metabolism. Graph shows the correlation between ALSFRS-R Gross Motor score (x axis) and the average SPM hyper-metabolism contrast values in the cerebellar cluster (y axis) (*right panel*). Positive SPM contrast values (y axis) indicate higher-than-HC brain glucose metabolism, and vice-versa. *Red shaded areas* represent confidence intervals for the regression line slope. Statistical threshold was set at $p < 0.001$ (uncorrected for multiple comparisons), with minimum cluster extent k:100 voxels. Only clusters surviving cluster-level FWE-correction are shown, rendered on a high-resolution anatomical template in MRIcron

identification of disease-specific brain hypometabolism patterns at the single-subject level in multiple neurodegenerative conditions (cfr. [61]), including movement disorder diseases [20, 26]. In the current study, however, no alterations in regional metabolism were sensitive and/or specific enough to provide an accurate discrimination between spinal- and bulbar-onset subtypes at the single-subject level (AUCs<0.63). Of note, these results were confirmed also when adopting two different multivariate approaches, with unsatisfactory AUC values (<.60), obtained following cross-validation. Our results therefore strongly suggest that no clear distinction between ALS variants can be provided by brain

metabolic patterns at the single-subject level. Crucially, the lack of definite metabolic patterns for ALS sub-types was driven by the striking metabolic variability, as provided by the regional hypo- and hyper-metabolism single-subject SPM-t-maps (Figs. 1 and 2). Previous evidence of variability in ALS hypo- and hyper-metabolism patterns is limited, but increasing. Van Laere et al. (2014) reported a certain variability in ALS metabolic profiles in 70 patients, though not affecting accurate discrimination between ALS and control cases. Crucially, the same was not true for differential diagnosis between ALS and PMA (with cross-validated accuracy dropping from 89.7% to 62.4%), although the low number of included PMA cases suggests caution in interpreting this finding [30]. Recently, Matias-Guiu and colleagues (2016) reported heterogeneous brain metabolism patterns in a small case series (N = 18) with frontal, parietal and temporal areas being variably involved; when clustering the individual hypo-metabolism patterns, they found that roughly one third of the patients showed a prevalent frontal hypo-metabolism, one third a more posterior pattern with prevalent motor and parietal involvement, and the remaining cases a mixed or negative pattern [31]. It has been hypothesized that presence of different metabolic patterns might be related to the pathological and clinical heterogeneity of ALS [31]. Accordingly, different patterns of TDP-43 pathology have been described in sporadic ALS at *postmortem* evaluation, in association to distinct clinical/cognitive profiles and patterns of neuronal loss [62, 63]. From the clinical standpoint, age of onset, relative mix of UMN and LMN signs and disease duration might contribute to more or less subtle differences in the clinical phenotype [64], with clinical variability mirrored by the heterogeneity of brain metabolic patterns. It stands to reason that presence of cognitive impairment might be a fundamental determinant of brain metabolic heterogeneity in ALS [32]. To this regard, a typical frontal hypo-metabolism pattern has been observed in ALS in association with fronto-temporal dementia and also to mild cognitive impairment, both at group- [32] and single-subject level [31]. Together with the high prognostic value shown by [18F]FDG-PET (combined with appropriate metrics) in the preclinical dementia phases (e.g. [21–23, 25, 27]), this evidence advocates for the need of further studies validating [18F]FDG-PET as a biomarker of dementia progression in ALS, crucially at the single-subject level [65].

Clinical-metabolic correlations

We showed that gross motor deficits are associated with key components of the brain motor circuits, with differences across ALS variants (Fig. 3). The finding of a significant association between primary motor cortex hypo-metabolism and severity of motor deficits in spinal-onset ALS is in accordance with the large body of evidence, in ALS, of decreased metabolism in primary motor cortex depending on clinical symptom progression [48, 66] and, notably, regardless of clinical signs of LMN degeneration [48]. Conversely, in bulbar-onset ALS, gross motor symptomatology was specifically associated with hyper-metabolism in cerebellar cortex and vermis, here reported for the first time. It is well-known that massive interconnections exist between cerebellum and primary motor cortex [67] and that cerebellum is organized according to a specific motor topography [68]. It is worth nothing that hemispheric lobules VIIb and IX are specifically involved during upper- and lower-limb movements [68], a result that fits well with the here reported association between hyper-metabolism in these specific cerebellar regions and gross motor impairment in activities such as walking, climbing stairs and turning in bed, as measured by ALSFRS-R. The involvement of the cerebellar cortex in the pathophysiology of gross motor symptoms is consistent with previous findings of increased cerebellar recruitment reported in ALS patients performing motor tasks and in functional connectivity rs-fMRI studies, showing increased connectivity along cerebellar-motor cortex loops, possibly suggestive of compensatory processes (cfr. [69]). Future studies will need to investigate the metabolic correlates of neuropsychological deficits in ALS, thus complementing our results on motor impairment.

We acknowledge that results of the assessment of the primary motor cortex are limited, taking into account both the anatomical characteristics of the primary motor cortex in MNI space and the relatively limited spatial resolution of PET. In particular, limits exist in studying small portions of the primary motor cortex, also located adjacently to one another, with risk of biases due to partial volume/spillover effects. Future studies, eventually combining high resolution structural MRI and [18F]FDG-PET are needed to address this important issue.

Conclusions

The observed large inter-subject variability in brain glucose metabolism alterations in ALS strongly undermines its potential value for differential diagnosis. The low accuracy level, obtained with both univariate and multivariate approaches, does not support the inclusion of [18F]FDG-PET in the routine diagnostic work-up for discrimination of ALS sub-syndromes, for the accuracy of which neurological and neurophysiological examinations remain the standard of truth. This conclusion is consistent with the recent recommendations promoted by an expert panel (referring to the European Association of Nuclear Medicine (EANM) and the European Academy of Neurology (EAN)) [33], that, after evaluating all available [18F]FDG-PET evidence in ALS, has suggested that metabolic abnormalities do not allow for a firm diagnosis of ALS. Still, [18F]FDG-PET might be useful for research purposes. To this regard, in this large case series, we observed syndrome-specific associations between clinical functional

motor scores and regional alterations of brain glucose metabolism, at group level, suggesting that different clinical onsets could be associated with different neurodegeneration pathways. Further studies will have to assess the functional relevance of metabolic changes in ALS for disease staging and monitoring.

Funding This study was funded by the Italian Ministry of Health (Ricerca Finalizzata Progetto Reti Nazionale AD NET-2011-02346784) (D.P), EU FP7 INMIND Project (FP7-HEALTH-2011-two-stage "Imaging of Neuroinflammation in Neurodegenerative Diseases", grant agreement no. 278850)" (D.P.), "IVASCOMAR project "Identificazione, validazione e sviluppo commerciale di nuovi biomarcatori diagnostici prognostici per malattie complesse" (grant agreement no. CTN01_00177_165430)" (D.P.), CARIPLO Project "Evaluation of autonomic, genetic, imaging and biochemical markers for Parkinson-related dementia: longitudinal assessment of a PD cohort" 2016–2020 (grant agreement no. 2014–0832)" (D.P.), Fondazione Eli-Lilly (Eli-Lilly grant 2011 "Imaging of neuroinflammation and neurodegeneration in prodromal and presymptomatic Alzheimer's disease phases")(C.C.), Ministero dell'Istruzione, dell'Università e della Ricerca – MIUR project "Dipartimenti di Eccellenza 2018–2022″ to Department of Neuroscience "Rita Levi Montalcini"(Ad.C, And.C, Ant.C.). This work was in part supported by the Italian Ministry of Health (Ricerca Sanitaria Finalizzata 2010, grant RF-2010e2309849) (Ad.C), the European Community's Health Seventh Framework Programme (FP7/2007–2013 under grant agreement 259867) (Ad.C), the Joint Programme - Neurodegenerative Disease Research (Italian Ministry of Education, University and Research) (Sophia) (Ad.C.), Fondazione Vialli e Mauro (And.C.); and Fondazione Magnetto (Ant.C.).

Compliance with ethical standards

Conflict of interest A. Chiò reports grants from the Italian Ministry of Health (Ricerca Finalizzata), EU JPND through the Ministry of Education, University, and Research, and the Italy-Israel Scientific Collaboration through the Italian Foreign Ministry, as well as personal fees from Biogen Idec, Cytokinetics, Italfarmaco, Mitsubishi Tanabe, and Neuraltus. All other authors declare that they have no conflict of interest.

Ethical approval All procedures performed in studies involving human participants were in accordance with the ethical standards of the institutional and/or national research committee and with the 1964 Helsinki declaration and its later amendments or comparable ethical standards.

Informed consent Informed consent was obtained from all individual participants included in the study.

References

1. Chiò A, Pagani M, Agosta F, Calvo A, Cistaro A, Filippi M. Neuroimaging in amyotrophic lateral sclerosis: insights into structural and functional changes. Lancet Neurol. 2014;13:1228–40.
2. Ludolph A, Drory V, Hardiman O, Nakano I, Ravits J, Robberecht W, et al. A revision of the El Escorial criteria - 2015. Amyotroph Lateral Scler Front Degener. 2015;16:291–2.
3. Brooks BR, Miller RG, Swash M, Munsat TL. El Escorial revisited: revised criteria for the diagnosis of amyotrophic lateral sclerosis. Amyotroph Lateral Scler Other Motor Neuron Disord. 2000;1:293–9.
4. Zoccolella S, Beghi E, Palagano G, Fraddosio A, Samarelli V, Lamberti P, et al. Predictors of delay in the diagnosis and clinical trial entry of amyotrophic lateral sclerosis patients: a population-based study. J Neurol Sci. 2006;250:45–9.
5. Turner MR, Kiernan MC, Leigh PN, Talbot K. Biomarkers in amyotrophic lateral sclerosis. Lancet Neurol. Elsevier Ltd. 2009;8:94–109.
6. Swinnen B, Robberecht W. The phenotypic variability of amyotrophic lateral sclerosis. Nat. Rev. Neurol. Nature Publishing Group. 2014;10:661–70.
7. Chiò AISIS. Survey: an international study on the diagnostic process and its implications in amyotrophic lateral sclerosis. J Neurol. 1999;246:1–5.
8. Belsh JM, Schiffman PL. The amyotrophic lateral sclerosis (ALS) patient perspective on misdiagnosis and its repercussions. J Neurol Sci. 1996;139:110–6.
9. Nzwalo H, De Abreu D, Swash M, Pinto S, De Carvalho M. Delayed diagnosis in ALS: the problem continues. J Neurol Sci. 2014;343:173–5.
10. Hardiman O, van den Berg LH, Kiernan MC. Clinical diagnosis and management of amyotrophic lateral sclerosis. Nat Rev Neurol Nature Publishing Group. 2011;7:639–49.
11. Dubois B, Feldman HH, Jacova C, Hampel H, Molinuevo JL, Blennow K, et al. Advancing research diagnostic criteria for Alzheimer's disease: the IWG-2 criteria. Lancet Neurol. 2014;13:614–29.
12. McKhann GM, Knopman DS, Chertkow H, Hyman BT, Jack CR, Kawas CH, et al. The diagnosis of dementia due to Alzheimer's disease: recommendations from the National Institute on Aging-Alzheimer's association workgroups on diagnostic guidelines for Alzheimer's disease. Alzheimer's dement. Elsevier Ltd. 2011;7:263–9.
13. McKeith I, Boeve B, Dickson D, Lowe J, Emre M, Al E. Diagnosis and management of dementia with Lewy bodies: fourth consensus report of the DLB consortium. Neurology. 2017;89:88–100.
14. Albert MS, DeKosky ST, Dickson D, Dubois B, Feldman HH, Fox NC, et al. The diagnosis of mild cognitive impairment due to Alzheimer's disease: recommendations from the National Institute on Aging and Alzheimer's association workgroup. Alzheimers Dement. 2011;7:270–9.
15. Gorno-Tempini ML, Hillis AE, Weintraub S, Kertesz A, Mendez M, Cappa SF, et al. Classification of primary progressive aphasia and its variants. Neurology. 2011;76:1006–14.
16. Rascovsky K, Hodges JR, Knopman D, Mendez MF, Kramer JH, Neuhaus J, et al. Sensitivity of revised diagnostic criteria for the behavioural variant of frontotemporal dementia. Brain. 2011;134:2456–77.
17. Stoessl AJ. Glucose utilization: still in the synapse. Nat Neurosci Nature Publishing Group. 2017;20:382–4.
18. Sperling RA, Aisen PS, Beckett LA, Bennett DA, Craft S, Fagan AM, et al. Toward defining the preclinical stages of Alzheimer's disease: recommendations from the National Institute on Aging-Alzheimer's association workgroups on diagnostic guidelines for Alzheimer's disease. Alzheimer's dement. Elsevier Ltd. 2011;7:280–92.
19. Armstrong MJ, Litvan I, Lang AE, Bak TH, Bhatia KP, Borroni B, et al. Criteria for the diagnosis of corticobasal degeneration. Neurology. 2013;80:496–503.
20. Caminiti SP, Alongi P, Majno L, Volontè MA, Cerami C, Gianolli L, et al. Evaluation of an optimized [18F]fluoro-deoxy-glucose positron emission tomography voxel-wise method to early support

differential diagnosis in atypical Parkinsonian disorders. Eur J Neurol. 2017;24:687–e26.
21. Cerami C, Dodich A, Greco L, Iannaccone S, Magnani G, Marcone A, et al. The role of single-subject brain metabolic patterns in the early differential diagnosis of primary progressive aphasias and in prediction of progression to dementia. J Alzheimers Dis. 2016;55: 183–97.
22. Perani D, Della Rosa PA, Cerami C, Gallivanone F, Fallanca F, Vanoli EG, et al. Validation of an optimized SPM procedure for FDG-PET in dementia diagnosis in a clinical setting. NeuroImage. Clin. Elsevier BV. 2014;6:445–54.
23. Perani D, Cerami C, Caminiti SP, Santangelo R, Coppi E, Ferrari L, et al. Cross-validation of biomarkers for the early differential diagnosis and prognosis of dementia in a clinical setting. Eur J Nucl Med Mol Imaging. 2016;43:499–508.
24. Cerami C, Della Rosa PA, Magnani G, Santangelo R, Marcone A, Cappa SF, et al. Brain metabolic maps in mild cognitive impairment predict heterogeneity of progression to dementia. NeuroImage Clin Elsevier BV. 2015;7:187–94.
25. Caminiti SP, Ballarini T, Sala A, Cerami C, Presotto L, Santangelo R, et al. FDG-PET and CSF biomarker accuracy in prediction of conversion to different dementias in a large multicentre MCI cohort. NeuroImage Clin Elsevier. 2018;18:167–77.
26. Pilotto A, Premi E, Caminiti SP, Presotto L, Alberici A, Paghera B, et al. Single-subject SPM FDG-PET patterns predict risk of dementia progression in Parkinson's disease. Neurology. 2018;90:e1029–37.
27. Iaccarino L, Chiotis K, Alongi P, Almkvist O, Wall A, Cerami C, et al. A cross-validation of FDG- and amyloid-PET biomarkers in mild cognitive impairment for the risk prediction to dementia due to Alzheimer's disease in a clinical setting. J Alzheimers Dis. 2017:1–12.
28. Pagani M, Chiò A, Valentini MC, Öberg J, Nobili F, Calvo A, et al. Functional pattern of brain FDG-PET in amyotrophic lateral sclerosis. Neurology. 2014;83:1067–74.
29. Cistaro A, Valentini MC, Chiò A, Nobili F, Calvo A, Moglia C, et al. Brain hypermetabolism in amyotrophic lateral sclerosis: a FDG PET study in ALS of spinal and bulbar onset. Eur J Nucl Med Mol Imaging. 2012;39:251–9.
30. Van LK, Vanhee A, Verschueren J, De CL, Driesen A, Dupont P, et al. Value of 18fluorodeoxyglucose-positron-emission tomography in amyotrophic lateral sclerosis a prospective study. JAMA Neurol. 2014;71:553–61.
31. Matías-Guiu JA, Pytel V, Cabrera-Martín MN, Galán L, Valles-Salgado M, Guerrero A, et al. Amyloid- and FDG-PET imaging in amyotrophic lateral sclerosis. Eur J Nucl Med Mol Imaging. 2016;43:2050–60.
32. Canosa A, Pagani M, Cistaro A, Montuschi A, Iazzolino B, Fania P, et al. 18F-FDG-PET correlates of cognitive impairment in ALS. Neurology. 2015;86:44–9.
33. Agosta F, Altomare D, Festari C, Orini S, Gandolfo F, Boccardi M, et al. Clinical utility of FDG-PET in amyotrophic lateral sclerosis and Huntington disease. Eur J Nucl Med Mol Imaging. 2018;45: 1546–56.
34. Varrone A, Asenbaum S, Vander Borght T, Booij J, Nobili F, Någren K, et al. EANM procedure guidelines for PET brain imaging using [18F] FDG, version 2. Eur J Nucl Med Mol Imaging Springer. 2009;36:2103–10.
35. Della Rosa PA, Cerami C, Gallivanone F, Prestia A, Caroli A, Castiglioni I, et al. A standardized [(18)F]-FDG-PET template for spatial normalization in statistical parametric mapping of dementia. Neuroinformatics. 2014;12:575–93.
36. Gallivanone F, Della Rosa P, Perani D, Gilardi MC, Castiglioni I. The impact of different 18FDG PET healthy subject scans for comparison with single patient in SPM analysis. Q J Nucl Med Mol Imaging. 2017;6(1):115–32.
37. Tzourio-Mazoyer N, Landeau B, Papathanassiou D, Crivello F, Etard O, Delcroix N, et al. Automated anatomical labeling of activations in SPM using a macroscopic anatomical parcellation of the MNI MRI single-subject brain. NeuroImage. 2002;15:273–89.
38. Sallet J, Mars RB, Noonan MP, Neubert F-X, Jbabdi S, O'Reilly JX, et al. The organization of dorsal frontal cortex in humans and macaques. J Neurosci. 2013;33:12255–74.
39. Mayka MA, Corcos DM, Leurgans SE, Vaillancourt DE. Three-dimensional locations and boundaries of motor and premotor cortices as defined by functional brain imaging: a meta-analysis. NeuroImage. 2006;31:1453–74.
40. Tziortzi AC, Searle GE, Tzimopoulou S, Salinas C, Beaver JD, Jenkinson M, et al. Imaging dopamine receptors in humans with [11C]-(+)-PHNO: dissection of D3 signal and anatomy. NeuroImage. 2011;54:264–77.
41. Lancaster J, Rainey L, Summerlin J, Freitas C. Automated labeling of the human brain: a preliminary report on the development and evaluation of a forward-transform method. Hum Brain Mapp. 1997;5:238–42.
42. Lancaster JL, Woldorff MG, Parsons LM, Liotti M, Freitas CS, Rainey L, et al. Automated Talairach atlas labels for functional brain mapping. Hum Brain Mapp. 2000;10:120–31.
43. Maldjian JA, Laurienti PJ, Kraft RA, Burdette JH. An automated method for neuroanatomic and cytoarchitectonic atlas-based interrogation of fMRI data sets. NeuroImage. 2003;19:1233–9.
44. Diedrichsen J, Maderwald S, Küper M, Thürling M, Rabe K, Gizewski ER, et al. Imaging the deep cerebellar nuclei: a probabilistic atlas and normalization procedure. NeuroImage. 2011;54: 1786–94.
45. Pagani M, Öberg J, De Carli F, Calvo A, Moglia C, Canosa A, et al. Metabolic spatial connectivity in amyotrophic lateral sclerosis as revealed by independent component analysis. Hum Brain Mapp. 2016;37:942–53.
46. Cauda F, Giuliano G, Federico D, Sergio D, Katiuscia S. Discovering the somatotopic organization of the motor areas of the medial wall using low-frequency bold fluctuations. Hum Brain Mapp. 2011;32:1566–79.
47. Bennett CM, Wolford GL, Miller MB. The principled control of false positives in neuroimaging. Soc Cogn Affect Neurosci. 2009;4: 417–22.
48. Endo H, Sekiguchi K, Ueda T, Kowa H, Kanda F, Toda T. Regional glucose hypometabolic spread within the primary motor cortex is associated with amyotrophic lateral sclerosis disease progression: a fluoro-deoxyglucose positron emission tomography study. eNeurologicalSci. 2017;6:74–9.
49. Verstraete E, Veldink JH, Hendrikse J, Schelhaas HJ, Van Den Heuvel MP, Van Den Berg LH. Structural MRI reveals cortical thinning in amyotrophic lateral sclerosis. J Neurol Neurosurg Psychiatry. 2012;83:383–8.
50. Genç B, Jara JH, Lagrimas AKB, Pytel P, Roos RP, Mesulam MM, et al. Apical dendrite degeneration, a novel cellular pathology for Betz cells in ALS. Sci Rep Nature Publishing Group. 2017;7: 41765.
51. Baker MR. ALS—dying forward, backward or outward? Nat Rev Neurol. 2014;10:660–0.
52. Chou SM, Norris FH. Amyotrophic lateral sclerosis: lower motor neuron disease spreading to upper motor neurons. Muscle Nerve. 1993;16:864–9.
53. Eisen A, Weber M. The motor cortex and amyotrophic lateral sclerosis. Muscle Nerve. 2001;24:564–73.
54. Yamanaka K, Chun SJ, Boillee S, Fujimori-Tonou N, Yamashita H, Gutmann DH, et al. Astrocytes as determinants of disease progression in inherited amyotrophic lateral sclerosis. Nat Neurosci. 2008;11:251–3.

55. Philips T, Robberecht W. Neuroinflammation in amyotrophic lateral sclerosis: role of glial activation in motor neuron disease. Lancet Neurol Elsevier Ltd. 2011;10:253–63.
56. Turner MR, Cagnin A, Turkheimer FE, Miller CCJ, Shaw CE, Brooks DJ, et al. Evidence of widespread cerebral microglial activation in amyotrophic lateral sclerosis: an [11C](R)-PK11195 positron emission tomography study. Neurobiol Dis. 2004;15:601–9.
57. Schroeter M, Dennin MA, Walberer M, Backes H, Neumaier B, Fink GR, et al. Neuroinflammation extends brain tissue at risk to vital peri-infarct tissue: a double tracer [11C]PK11195- and [18F]FDG-PET study. J Cereb Blood Flow Metab. 2009;29:1216–25.
58. Turner MR, Kiernan MC. Does interneuronal dysfunction contribute to neurodegeneration in amyotrophic lateral sclerosis? Amyotroph Lateral Scler. 2012;13:245–50.
59. Sibson NR, Dhankhar A, Mason GF, Rothman DL, Behar KL, Shulman RG. Stoichiometric coupling of brain glucose metabolism and glutamatergic neuronal activity. Neurobiology. 1998;95:316–21.
60. Schreiber H, Gaigalat T, Wiedemuth-Catrinescu U, Graf M, Uttner I, Muche R, et al. Cognitive function in bulbar- and spinal-onset amyotrophic lateral sclerosis: a longitudinal study in 52 patients. J Neurol. 2005;252:772–81.
61. Iaccarino L, Sala A, Caminiti SP, Perani D. The emerging role of PET imaging in dementia. F1000Research. 2017;6:1830.
62. Takeuchi R, Tada M, Shiga A, Toyoshima Y, Konno T, Sato T, et al. Heterogeneity of cerebral TDP-43 pathology in sporadic amyotrophic lateral sclerosis: evidence for clinico-pathologic subtypes. Acta Neuropathol Commun Acta Neuropathologica Communications. 2016;4:61.
63. Nishihira Y, Tan CF, Onodera O, Toyoshima Y, Yamada M, Morita T, et al. Sporadic amyotrophic lateral sclerosis: two pathological patterns shown by analysis of distribution of TDP-43-immunoreactive neuronal and glial cytoplasmic inclusions. Acta Neuropathol. 2008;116:169–82.
64. Sabatelli M, Conte A, Zollino M. Clinical and genetic heterogeneity of amyotrophic lateral sclerosis. Clin Genet. 2013;83:408–16.
65. Willekens SMA, Van Weehaeghe D, Van Damme P, Van Laere K. Positron emission tomography in amyotrophic lateral sclerosis: towards targeting of molecular pathological hallmarks. Eur J Nucl Med Mol Imaging. 2016:1–15.
66. Hoffman JM, Mazziotta JC, Hawk TC, Sumida R. Cerebral glucose utilization in motor neuron disease. Arch Neurol. 1992;49:849–54.
67. Buckner RL. The cerebellum and cognitive function: 25 years of insight from anatomy and neuroimaging. Neuron. 2013;80:807–15.
68. Mottolese C, Richard N, Harquel S, Szathmari A, Sirigu A, Desmurget M. Mapping motor representations in the human cerebellum. Brain. 2013;136:330–42.
69. Prell T, Grosskreutz J. The involvement of the cerebellum in amyotrophic lateral sclerosis. Amyotroph Lateral Scler Front Degener. 2013;14:507–15.